

This article was downloaded by:

On: 30 January 2011

Access details: *Access Details: Free Access*

Publisher *Taylor & Francis*

Informa Ltd Registered in England and Wales Registered Number: 1072954 Registered office: Mortimer House, 37-41 Mortimer Street, London W1T 3JH, UK



## Separation & Purification Reviews

Publication details, including instructions for authors and subscription information:

<http://www.informaworld.com/smpp/title~content=t713597294>

### Theory of Simultaneous Multiple Streak Collimation in Continuous-Flow Electrophoresis by Superposition of Electro-Osmosis and Thermal Convection

Alexander Kolin<sup>a</sup>; Brent L. Ellerbroek<sup>b</sup>

<sup>a</sup> Molecular Biology Institute University of California, Los Angeles, California <sup>b</sup> Department of Mathematics California, Institute of Technology, Pasadena, California

**To cite this Article** Kolin, Alexander and Ellerbroek, Brent L.(1979) 'Theory of Simultaneous Multiple Streak Collimation in Continuous-Flow Electrophoresis by Superposition of Electro-Osmosis and Thermal Convection', *Separation & Purification Reviews*, 8: 1, 1 – 19

**To link to this Article: DOI:** 10.1080/03602547908057228

**URL:** <http://dx.doi.org/10.1080/03602547908057228>

## PLEASE SCROLL DOWN FOR ARTICLE

Full terms and conditions of use: <http://www.informaworld.com/terms-and-conditions-of-access.pdf>

This article may be used for research, teaching and private study purposes. Any substantial or systematic reproduction, re-distribution, re-selling, loan or sub-licensing, systematic supply or distribution in any form to anyone is expressly forbidden.

The publisher does not give any warranty express or implied or make any representation that the contents will be complete or accurate or up to date. The accuracy of any instructions, formulae and drug doses should be independently verified with primary sources. The publisher shall not be liable for any loss, actions, claims, proceedings, demand or costs or damages whatsoever or howsoever caused arising directly or indirectly in connection with or arising out of the use of this material.

**THEORY OF SIMULTANEOUS MULTIPLE STREAK COLLIMATION IN  
CONTINUOUS-FLOW ELECTROPHORESIS BY SUPERPOSITION OF  
ELECTRO-OSMOSIS AND THERMAL CONVECTION**

by

Alexander Kolin  
Molecular Biology Institute  
University of California, Los Angeles, California

and

Brent L. Ellerbroek  
Department of Mathematics  
California Institute of Technology, Pasadena, California

**Introduction**

The resolving power in continuous flow streak deflection electrophoresis (the "free flow" curtain electrophoresis as well as in "endless fluid belt" electrophoresis) is limited by the broadening of the streaks during the process of electro-migration. This effect becomes more pronounced as the diameter of the injector is increased to augment the throughput. A gain in the latter is thus achieved at a sacrifice in resolution. It has been possible until now to avoid this limitation for only one fraction of an electrophoretic mixture, namely that component whose electrophoretic velocity is equal and opposite to the velocity of the electro-osmotic flow adjacent to the wall of the electrophoretic curtain (6,7). This paper elucidates a way to achieve streak collimation (i.e. elimination of streak broadening) simultaneously for all components of an electrophoretic mixture and to do it in an optimal velocity configuration where the throughput increases with the square of the injector diameter without an essential concomitant loss in resolution.

### The Problem of Streak Broadening due to Mismatching of Orthogonal Velocity Profiles

The present theory holds for all forms of continuous-flow streak deviation electrophoresis. This includes "free flow" (1) fluid curtain- and endless fluid belt electrophoresis (2). For simplicity, we shall consider a flat vertical fluid curtain flowing downward between two parallel vertical plates whose separation is negligible as compared to their vertical and horizontal dimensions. The flowing fluid will be an aqueous solution above 4° C. Typically, the distance  $h$  between the plates will be 1.5 mm and the central downward velocity in the laminar velocity distribution in the order of 4 mm/sec.

We imagine the plates to be parallel to the page and the buffer solution between them to be traversed by a horizontal current establishing a horizontal electric field. A solution containing negative colored ions is injected from a narrow slit which is perpendicular to the plates so that a narrow colored band (as wide as the gap between the plates) forms a narrow rectangular descending streak in the downward laminar flow. This situation is illustrated in Fig. 1 in the straight flow section between the levels  $L_1$  and  $L_2$  where AB is the slit through which the streak of ions enters.

In the absence of an electric field the streak will follow a straight path indicated by the line D. A horizontal electric field will move the negative ions to the left toward the anode with a velocity independent of the coordinate  $z$ . If the downward flow velocity were uniform, the streak originating from Level  $L_1$  at AB would terminate at level  $L_2$  intersecting this plane along a straight line  $A^*B^*$ . Actually, however, the vertical velocity profile is parabolic as shown in Fig. 1. As a result of this, the fluid elements originating at points  $l \neq r$  near the rear and front walls R and F which confine the fluid belt will move downward more slowly than the central fluid elements emanating from point 0. They will remain in the electric field on their way to their terminal points  $l^*m^*q^*r^*$  longer than the central streak and will be consequently deviated further to the left by the time they reach the level  $L_2$ . Thus, the originally straight cross-section of the ion band will be deformed as indicated at level  $L_2$  by the curved band  $l^*m^*n^*o^*p^*q^*r^*$ . If the collector COL consists of straight slots, as shown at level  $L_2$  in Fig. 1, this electrophoretically homogeneous component will not be collected through one slot in the fraction collector, but rather, through many slots, which constitutes a serious impairment of preparative resolution.

Visual observation of streak separations will also be impaired for streaks of circular cross-section emanating from injection port C, at level  $L_1$ . Due to the effect described above ("parabolic divergence") the centrally located ions will suffer the smallest deviation while the ones closest to the walls R and F will move farthest to the left and the streak cross-section will be distorted into the crescent  $C_2$  at level  $L_2$ . Since a faster electrophoretic component may be located as indicated by crescent  $C_3$  at level  $L_2$  its trailing edge may be located between the "horns" of the crescent  $C_2$  so that the two actually separated streaks may appear as one broad streak when viewed from the side (2,3).

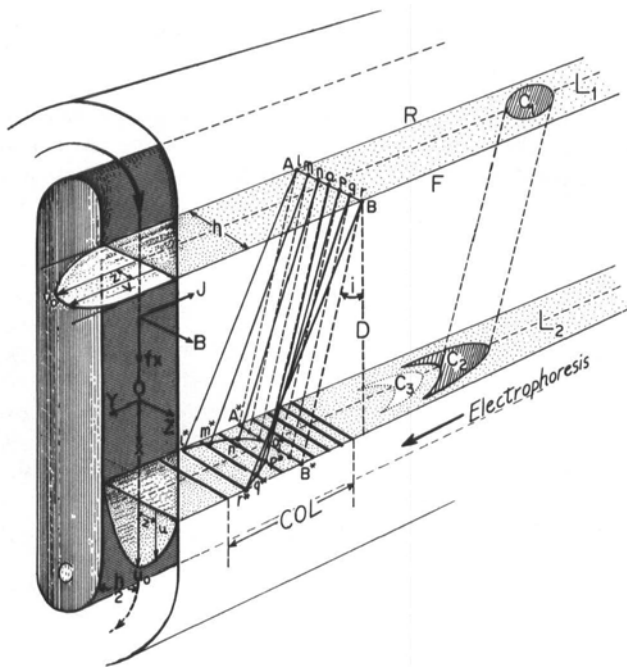


Fig. 1 Iron core C with surrounding buffer belt of an endless belt electrophoresis apparatus. R, F.: rear and front boundaries, respectively, of the buffer belt.  $L_1$ ,  $L_2$ : two levels in the front section of an endless belt. Vertical and horizontal parabolas show the vertical and horizontal profiles of laminar flows.  $\vec{J}_0$ ,  $\vec{v}_0$ : central flow velocities. B, J,  $f_x$ : vectors of magnetic field, current density and vertical force density, respectively. C<sub>1</sub>: circular cross-section of a streak entering the fluid curtain at level  $L_1$ . C<sub>2</sub>: distorted streak cross-section downstream at level  $L_2$ . C<sub>3</sub>: Streak cross-section of a component faster than that corresponding to C<sub>2</sub>. BD: perpendicular to planes  $L_1$  and  $L_2$ . AB: narrow slit on level  $L_1$ . Col: collector (From A. Kolin: in *Methods of Cell Separation* Vol. 2, N. Catsimpoolas, Ed. Plenum Publ. Co., New York, 1979).

#### Avoidance of Streak Distortion in Matched Velocity Profiles

It has been pointed out (2,3,4) that the distortion of the streak profile described above will not occur if the velocity distributions of the downward and lateral motions of the charged particles are the same. Thus, if the lateral velocity distribution is parabolic as shown in Fig. 1 at level  $L_1$  as well as the vertical velocity profile seen at level  $L_2$ , all particles in the streak, regard-

less of their coordinate  $z$  values, will suffer the same angular deviation  $\alpha$  and the original cross-section of the streak will remain preserved during electromigration.

The same will happen in the ideal case where the velocity distributions in the vertical and horizontal flow are uniform. In this case, the superposition of a uniform horizontal velocity of electrophoresis on the uniform horizontal flow will not result in a mismatching of the velocity profiles and the consequent streak distortion.

#### Rectification of the Horizontal Velocity Profile by Electro-osmosis

In a closed system (at zero net horizontal fluid transfer), electro-osmotic convection will be engendered due to interaction between the ions in the ionic atmosphere adjacent to the cell walls and the electric field. The resultant streaming pattern and velocity distribution is shown in Fig. 2. The fluid motion near the walls is opposite to that near the center of the fluid belt between the closely spaced parallel plates. The relation between the velocity  $v_w$  at the walls and the central velocity  $v_o$  is  $v_w = -2v_o$ . The convection pattern is a double circulation shown by dashed lines. There are two planes  $z_1$  and  $z_2$  in which the velocity  $v$  vanishes. They are located at the distance  $0.21h$  from the walls  $P_1$  and  $P_2$  (2,3,5).

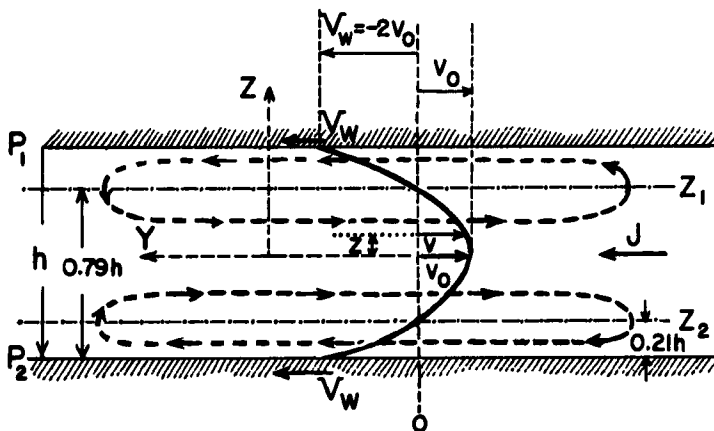


Fig. 2 Electro-osmotic velocity distribution.  $P_1, P_2$ : parallel plates separated by distance  $h$ .  $J$ : electrical current density.  $Z_1, Z_2$ : Smoluchowski zones of zero velocity.  $v_o$ : central velocity  $v_w = -2v_o$ : wall velocity. Closed dashed lines depict electro-osmotic convection. (From A. Kolin in Methods of Cell Separation Vol. 2, N. Catsimpoolas, Ed. Plenum, Publ. Co. New York, 1979).

It has been shown (2,3,6) that the horizontal velocity profile can be modified by superposition of electrophoresis and electro-osmosis in such a fashion that the streak distortion will disappear for a particle of one particular electrophoretic mobility (namely, an electrophoretic mobility  $\mu$  equal and opposite to the electro-osmotic mobility  $W$  corresponding to the given cell wall in the given buffer.) Let us imagine, referring to Fig. 2, a species of ions migrating to the right with the velocity  $v_e = -v_w = 2v_0$  uniformly throughout the width  $h$  of the fluid. We see that this motion shifts the value of the velocity near the wall to  $v = 0$  and the parabolic velocity distribution becomes the same as that of the descending laminar flow in the fluid curtain. The vertical and horizontal velocities of the ions are now perfectly matched for each value of  $z$  so that their ratio is constant over the entire width  $h$  of the fluid curtain and the "crescent" streak distortion is eliminated for ions whose electrophoretic velocity happens to be equal to the electro-osmotic wall velocity (6).

This is, however, a haphazard advantage in analytical work. It is essential to be able to achieve this condition for any chosen electrophoretic component. It has been suggested to accomplish this by modification of the effective cell wall zeta potential (7). But, even if perfected to ideal performance, this method could only permit optimal preparative collection of one fraction at a time. A limitation of the advantage of this method of streak collimation is that the small fluid velocities near the walls result in only small increases in the throughput when the diameter of the injector is increased to the full width of the annulus.

#### Rectification of Velocity Profiles as a Method of Streak Collimation

In the preceding section we achieved streak collimation by matching the vertical and horizontal velocity profiles, making both of them parabolic. This resulted in streak rectification for only one electrophoretic component whose electrophoretic velocity coincided with the electro-osmotic wall velocity.

We shall now seek to modify both the horizontal and the vertical velocity profiles so as to make them uniform, at least over a large fraction of the width of the annulus. This will still be an application of the principle of matching of velocity profiles (2) but the choice of a uniform velocity distribution will have an important advantage. A superposition of a uniform electrophoretic velocity of the particles upon the horizontal uniform flow velocity will still yield a uniform velocity distribution matching the uniform vertical velocity profile. And this will be true for all electrophoretic components regardless of their mobility value. Thus, we should obtain simultaneous streak collimation for all electrophoretic components for this choice of velocity profiles. It now remains to be seen to what extent this can be achieved.

Rectification of the Horizontal Velocity Profile by Superposition of Electro-osmotic Streaming.

When we contemplate the electro-osmotic velocity profile shown in Fig. 2, it is easy to visualize that superposition of a laminar flow from right to left of a suitable magnitude could rectify the horizontal velocity profile. If the chosen parabolic flow has a central velocity  $v^* = -3 v_o$ , then the central velocity will become  $= -2 v_o$ , i.e. equal to the electro-osmotic wall velocity. Similarly, the velocity near the wall will remain  $= -2 v_o$  since the wall velocity of the superimposed laminar flow is  $= 0$ . The addition of the velocities at all intermediate points will result in  $v(z) = -2 v_o$  so that a uniform horizontal velocity profile will prevail over the entire width of the annulus.

Rectification of the Vertical Velocity Profile by Thermal Convection to Achieve Simultaneous Elimination of Streak Distortion for all Fractions.

We will now consider the thermal convection pattern which prevails between closely spaced parallel vertical plates between which a uniformly heated fluid is confined as in the case of the flowing curtain - and non-circular endless fluid belt electrophoresis. In view of the horizontal temperature gradient in a vertical uniformly heated sheet of fluid cooled through the confining parallel plates, a horizontal temperature gradient is set up in the fluid. The concomitant density gradient causes disequilibration resulting in a convection pattern where the fluid rises in the central region and descends near the cooling plates. This convection pattern (Fig. 3) is very similar to the electro-osmotic convection (dashed lines) shown in Fig. 2, except that we must rotate Fig. 2  $90^\circ$  so that  $v_o$  points upward and replace the vector  $\vec{J}$  by the gravitational field vector  $g$  to achieve the analogy. If the solid parabola were indeed the velocity distribution of thermal convection, the situation would be ideal for rectification of the velocity profile by superposition of a downward laminar flow (in analogy with our procedure used with the electro-osmotic flow). Unfortunately this analogy is only superficial since the thermal convection velocity must vanish at the walls. However, as is shown in the calculations presented below, the thermal convection velocity distribution at some distance from the walls is essentially parabolic thus permitting adequate rectification of the downward laminar flow profile over roughly half of the width of the fluid curtain. In Fig. 4 curve  $u(z)$  shows the correct calculated thermal convection velocity profile (9) in which the fluid is at rest near the walls moving upward with maximum velocity at the center and descending in two intermediate regions. The superposition of the thermal convection profile (curve  $u(z)$ ) upon a suitably proportioned laminar flow profile (curve  $w(z)$ ) results in a curve  $u(z) + w(z)$  which is close to a uniform velocity distribution over a large portion of the annulus width.

We are now ready to superimpose the rectified horizontal uniform velocity profile (achieved by superposition of a horizontal laminar flow upon electroosmotic streaming) extending over the entire width  $h$  of the annulus with

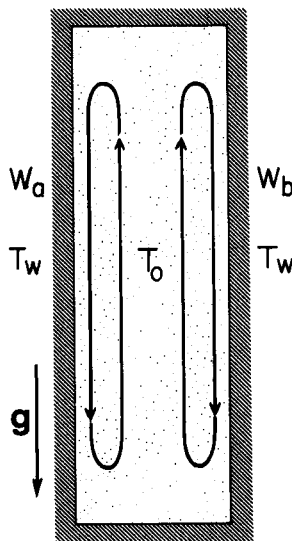


Fig. 3 Thermal convection pattern between adjacent parallel vertical plates ( $W_a$ ,  $W_b$ ) in a uniformly heated fluid.  $T_w$ : temperature of the vertical plates.  $T_0$ : temperature at the center of the fluid.  $\vec{g}$ : gravitational field vector.

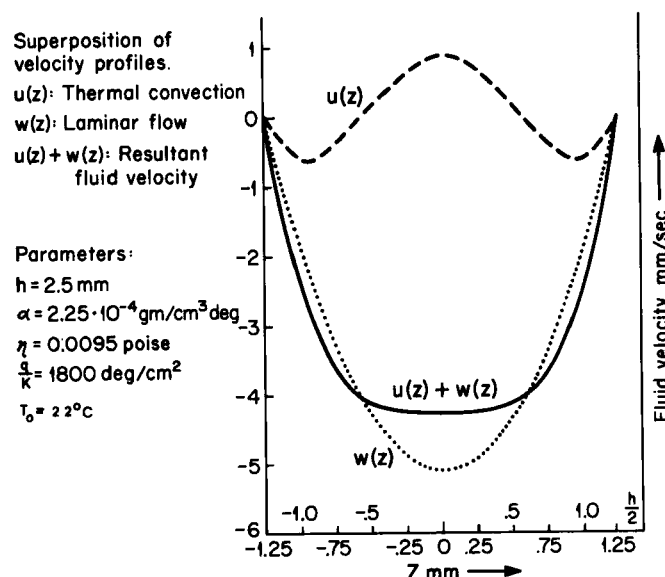


Fig. 4 Central rectification of the fluid velocity profile by superposition of a laminar flow ( $w(z)$ ) upon the thermal convection ( $u(z)$ ). The resulting velocity distribution  $u(z) + w(z)$  is flat over a wide span in the central region.

our vertical velocity profile ( $u(z) + w(z)$  in Fig. 4) which is rectified over an appreciable central region. Within this region we have conditions approaching the ideal situation of two orthogonal uniform flows which will produce no streak distortion when a uniform electrophoretic migration is imposed upon injected charged particles. It will be shown below that an increase in throughput of more than an order of magnitude can thus be achieved without impairment of resolution as compared to standard methods.

### Calculation of the Velocity Profile of Thermal Convection

#### Assumptions

A) The lateral dimensions of the plates are infinite as compared to their separation. B) Assumption (A) implies that temperature and velocity are functions of  $z$  only, where  $z$  is the distance from the mid-plane between the plates measured along the normal (see Fig. 1). C) We ignore fluid motion at infinity (i.e. at the edges of the plates). There is thus only vertical fluid motion (see Fig. 3). D) Due to absence of horizontal flow within the finite range, there is no horizontal convective heat transfer toward the heat sinks (the vertical plates). The above implies that heat transfer can occur horizontally by conduction only. E) The system is considered in a steady state. This implies the vanishing of all time derivatives and the equilibrium of all net forces. F) The fluid is bounded on all sides by rigid walls.

#### Derivation of the Velocity Distribution \*

We start with Fourier's differential heat equation

$$\nabla^2 T = - \frac{q}{k} = \frac{d^2 T}{dz^2} \quad (1)$$

Integrating twice we obtain

$$T = T_w + \frac{q}{8k} (h^2 - 4z^2) \quad (2)$$

(The first integration constant is  $A = 0$  because at the central temperature maximum  $(\frac{dT}{dz})_0 = 0$ . The second integration constant is the wall temperature

---

\* We are indebted to Prof. F. Busse of the UCLA Institute of Geophysics for below derivation.

$T_w$  at  $z = \frac{h}{2}$ . ) The density as a function of temperature is

$$\rho = \rho_0 [1 - \alpha (T - T_w)]. \quad (3)$$

The equation of motion is

$$\left( \frac{\partial}{\partial t} + \vec{u} \cdot \nabla \right) \vec{u} = - \nabla \frac{P}{\rho_0} - g \vec{\alpha} (T - T_w) + \eta \nabla^2 \vec{u}. \quad (4)$$

Assuming a steady-state flow,  $\frac{dp}{dx} = \text{constant}$ ,  $\vec{u} = u(z)$  and, neglecting the temperature dependence of the viscosity  $\eta$ , we obtain the solution of equation (4) as follows:

from equations (2) and (4)

$$\eta \frac{d^2 u(z)}{dz^2} = C + g \alpha (T - T_w) = C + g \alpha \frac{q}{8k} (h^2 - 4z^2). \quad (4a)$$

(Where  $C = \frac{\partial}{\partial x} \left( \frac{P}{\rho_0} \right)$  determines the rate of change of the pressure gradient due to heating). After two integrations

$$\eta u(z) = g \alpha \left( \frac{q}{8k} \right) \left( h^2 \frac{z^2}{2} - \frac{z^4}{3} \right) + C \frac{z^2}{2} + d. \quad (5)$$

In equations (4a) and (5), C and d stand for the following abbreviations

$$C = -g \alpha \frac{q}{10k} h^2 \quad (6)$$

and

$$d = -g \alpha \frac{q}{16k} \frac{h^4}{120} \quad (7)$$

(These constants are determined by the conditions of  $u(z) = 0$  at the walls

$(z = \pm \frac{h}{2})$  and of conservation of mass:  $\int_{-\frac{h}{2}}^{\frac{h}{2}} u(z) dz = 0$  (zero net vertical

mass transfer.) These conditions yield from equation (5) two equations in the unknowns C and d from which the values given in equations (6) and (7) follow by straightforward algebra.

Substitution of the values of C and d from equations (6) and (7) in equation (5) yields the velocity distribution of thermal convection

$$u(z) = \frac{g \alpha q}{80k\eta} \left\{ h^2 z^2 - \frac{10}{3} z^4 - \frac{h^4}{24} \right\} \quad (8)$$

### Discussion of the Solution

Equation (8) shows that it is the temperature coefficient of density, rather than the density proper that determines the magnitude of the thermal convection.

Like in the case of electro-osmotic convection, there are two planes of zero velocity whose coordinates are

$$z_1 = + \frac{h}{2\sqrt{5}} \quad \text{and} \quad z_2 = - \frac{h}{2\sqrt{5}} \quad ,$$

whereas the coordinates of the corresponding planes in electro-osmosis are

$$+ \frac{h}{2\sqrt{3}} \quad \text{and} \quad - \frac{h}{2\sqrt{3}} \quad .$$

The maximum of the upward velocity is at the center ( $z = 0$ ). The positions of the downward velocity maxima are at

$$z_a = \frac{h}{2} \sqrt{\frac{3}{5}} \quad z_b = - \frac{h}{2} \sqrt{\frac{3}{5}} \quad .$$

The maximum downward velocity is  $u_d = - \frac{5}{6} u_o$ .

The magnitude of the maximum upward velocity at  $z = 0$  is

$$u_o = \frac{g \alpha q}{80k \eta} \left( \frac{h^4}{24} \right) \quad . \quad (9)$$

### Superposition of the Vertical Laminar Velocity Profile upon Thermal Convection

The vertical laminar flow is described by

$$w(z) = w_o \left( 1 - 4 \left( \frac{z}{h} \right)^2 \right) \quad (10)$$

(see curve  $w(z)$  in Fig. 4).

The resultant velocity distribution in a superposition of downward laminar flow  $w(z)$  upon thermal convection follows from equations (8), (9) and (10) :

$$R(z) = u(z) + w(z) = A \left[ \left( \frac{z}{h} \right)^2 - \frac{10}{3} \left( \frac{z}{h} \right)^4 - \frac{1}{24} \right] + w_o \left[ 1 - 4 \left( \frac{z}{h} \right)^2 \right] \quad (11)$$

(where we write  $A = \frac{g \alpha q h^4}{80 k \eta}$ ).

To find conditions for maximum flow uniformity in the central region, we neglect the  $z^4$  term in equation (II) which is small in that region and choose such a value ( $w_o^*$ ) for the central maximum velocity  $w_o$  of the vertical laminar flow that the  $z^2$  terms in the thermal convection and laminar flow terms of equation (II) cancel each other. Thus the curvature-determining  $z^2$  term is reduced to zero and we obtain:

$$R(z) = u(z) + w(z) \approx A \left[ \left( \frac{z}{h} \right)^2 - \frac{1}{24} \right] + w_o^* \left[ 1 - 4 \left( \frac{z}{h} \right)^2 \right] = \\ = \left( \frac{z}{h} \right)^2 \left[ A - 4 w_o^* \right] - \frac{A}{24} + w_o^* = w_o^* - \frac{A}{24} . \quad (II)$$

The  $z^2$  term vanishes for

$$w_o^* = \frac{g \alpha q h^4}{320 k \eta} . \quad (III)$$

The relation between central velocities of the critical laminar flow ( $w_o^*$ ) and thermal convection ( $u_o$ ) is from equations (9) and (III)

$$\frac{w_o^*}{u_o} = 6 . \quad (IV)$$

Since  $A = 4 w_o^*$ , equation (II) can be written as follows for the condition  $w_o = w_o^*$

$$R(z) = w_o^* \left\{ 4 \left[ \left( \frac{z}{h} \right)^2 - \frac{10}{3} \left( \frac{z}{h} \right)^4 - \frac{1}{24} \right] + \left[ 1 - 4 \left( \frac{z}{h} \right)^2 \right] \right\} , \quad (IIa)$$

whence follows

$$R(z) = \frac{5}{6} w_o^* \left[ 1 - \left( \frac{2z}{h} \right)^4 \right] , \quad (IIb)$$

or in terms of  $g$ ,  $\alpha$ ,  $q$ ,  $\eta$ , and  $k$ :

$$R(z) = \frac{g \alpha q}{24 k \eta} \left[ \left( \frac{h}{2} \right)^4 - z^4 \right] . \quad (IIb)$$

The term in front of the parenthesis in equation (IIb) has the meaning of the maximum velocity  $R_o = R(0)$  at  $z = 0$  in the rectified velocity distribution described by equations (II) a and b. We can thus write for the velocity profile of the rectified flow

$$R(z) = R_0 \left[ 1 - \left( \frac{2z}{h} \right)^4 \right] \quad , \quad (15a)$$

where

$$R_0 = R(0) = \frac{5}{6} w_0^* = \frac{g \alpha q \left( \frac{h}{2} \right)^4}{24 k \eta} \quad . \quad (15b)$$

### Evaluation of the Improvement in Streak Collimation by Rectification of the Velocity Profile

The streak divergence in a vertical fluid curtain can be easily visualized as follows. A vertical cylindrical injector of diameter  $d = 2z$  is centered within the fluid curtain (or annulus) of width  $h$  so that its axis is centered within the curtain's mid-plane at  $z = \frac{h}{2}$ . In a vertical laminar flow, for instance, particles escaping from the injector along its center axis at  $z = 0$  will have the highest downward velocity  $w_0$  and, consequently, will suffer the smallest lateral deviation  $\alpha_1$  due to electromigration with the velocity  $v = \mu E$ . All other particles located in planes  $z \neq 0$  will have smaller vertical velocities in the laminar flow profile and will, since they migrate laterally with the same velocity  $v = \mu E$ , suffer a greater angular deviation  $\alpha_2$ . Thus, centrally located particles will form the trailing edge of the streak which emanates from the injector and the particles leaving the injector at points of  $z = \frac{h}{2}$  will form the leading edge of the streak. There will thus be an angle of divergence between the leading and trailing edge of the streak given by  $\alpha = \alpha_2 - \alpha_1$ . We shall adopt  $\tan \alpha$  as a measure of streak divergence. Using a trigonometric transformation, we write

$$\tan \alpha = \tan (\alpha_2 - \alpha_1) = \frac{\tan \alpha_2 - \tan \alpha_1}{1 + \tan \alpha_2 \tan \alpha_1} \quad . \quad (16)$$

Since  $\tan \alpha_1 = \frac{\mu E}{w_0}$  and  $\tan \alpha_2 = \frac{\mu E}{w}$  we obtain

$$\tan \alpha = \frac{\frac{\mu E}{w} - \frac{\mu E}{w_0}}{1 + (\mu E)^2 / w_0 w} \quad . \quad (17)$$

Assuming the electrophoretic velocity  $\mu E$  to be much smaller than the vertical curtain flow velocity ( $\mu E$ )<sup>2</sup>  $\ll w w_0$ , we obtain

$$\tan \alpha \approx \mu E \frac{w_o - w}{w_o w} \equiv \frac{\Delta}{100} \quad , \quad (18)$$

where  $\Delta$  measures the slope of the streak divergence in %.

We shall now compare the streak divergence in a parabolic flow given by equation (10) and a rectified flow described by equation (15a). We will assume for the sake of comparison the two flows to have the same central maximum velocity  $w_o = R_o$ .

Substituting the expression for  $w$  from equation (10) in equation (18) and designating the streak divergence as  $\Delta'$ , we obtain for parabolic flow

$$\frac{\Delta'}{100} = \mu E \frac{w_o - w_o \left[ 1 - \left( \frac{2z}{h} \right)^2 \right]}{w_o w} = \frac{\mu E}{w_o \left[ \left( \frac{h}{2z} \right)^2 - 1 \right]} . \quad (19')$$

After a similar substitution of the values of  $R = R(z)$  and  $R(0) = R_o$  in equation (18) we obtain for the streak divergence in rectified flow under the same electrophoretic conditions

$$\frac{\Delta''}{100} = \mu E \frac{R_o - R_o \left[ 1 - \left( \frac{2z}{h} \right)^4 \right]}{R_o R} = \frac{\mu E}{R_o \left[ \left( \frac{h}{2z} \right)^4 - 1 \right]} . \quad (19'')$$

Equations (19') and (19'') enable us to plot the streak divergence as a function of injector width for a parabolic ( $\Delta'$ ) as well as for a rectified ( $\Delta''$ ) curtain flow profile as shown in Fig. 5. We see that the streak divergence is considerably smaller in rectified flow than in parabolic flow for all values of the injector width.

The degree of improvement in streak collimation, and thus in resolution, can be seen most easily from the "improvement ratio"  $i$ :

$$i = \frac{\Delta'}{\Delta''} = \frac{R_o}{w_o} \frac{\left[ \left( \frac{h}{2z} \right)^4 - 1 \right]}{\left[ \left( \frac{h}{2z} \right)^2 - 1 \right]} = \left[ \left( \frac{h}{2z} \right)^2 + 1 \right] \quad (20)$$

(since we assume  $R_o = w_o$  in this comparison). The curve for  $i$  in Fig. 5 indicates a very high improvement ratio at small values of the injector width and a decline for wider injectors. Table I summarizes values of  $\Delta'$ ,  $\Delta''$  and  $i$  for selected injector widths  $d$  expressed in terms of the width  $h$  of the annulus.

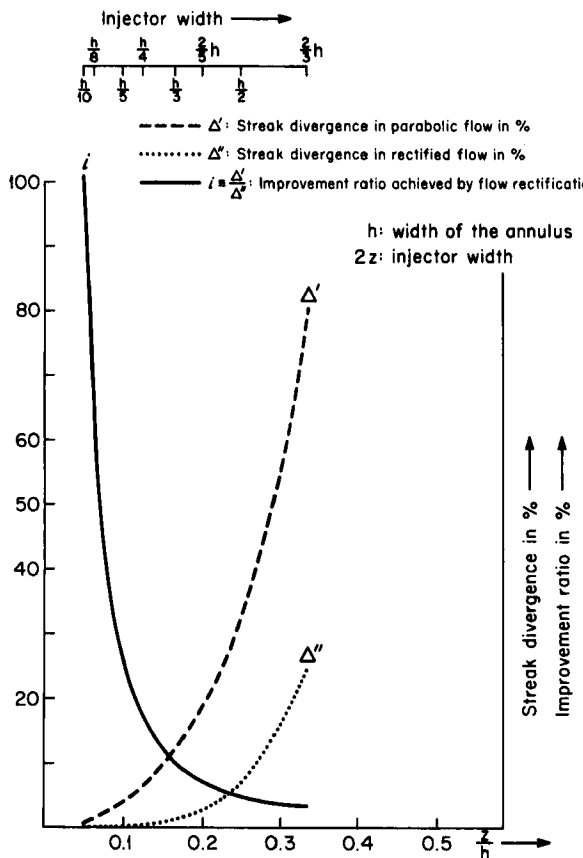


Fig. 5 Angular streak divergence in % for parabolic flow ( $\Delta'$ ) and for rectified flow ( $\Delta''$ ). The streak collimation by superposition of thermal convection is measured by the improvement ratio  $i = \Delta'/\Delta''$ . The lower scale measures the abscissa  $z$  in terms of the annulus width  $h$ . The upper horizontal scale permits the determination of  $\Delta'$ ,  $\Delta''$  and  $i$  for injectors of different width given as a fraction of the annulus width  $h$ .

#### Example of a Suitable Set of Instrumental Parameters

Until now the tendency has been to make the width of the annulus or fluid curtain as small as possible to suppress thermal convection. The possibility of rectification of the velocity profile with consequent increase in

Table I

<u>injector distance from midplane width</u>	<u><math>(\frac{h}{2z})</math></u>	<u><math>\left[ \left( \frac{h}{2z} \right) - 1 \right]^2</math></u>	<u><math>\left[ \left( \frac{h}{2z} \right) - 1 \right]^4</math></u>	<u><math>\gamma_{\Delta}^*</math></u> %	<u><math>\gamma_{\Delta''}^*</math></u> %	<u>rectified-flow divergence</u>	<u>improvement ratio</u>
$\frac{2}{3}h$	$h/3$	1.5	1.25	4.06	80	24.6	3.25
$\frac{1}{2}h$	$h/4$	2.0	3.0	15.0	33.3	6.67	5.00
$\frac{2}{5}h$	$h/5$	2.5	5.25	38.06	19.0	2.63	7.25
$\frac{1}{3}h$	$h/6$	3.0	8.0	80.0	12.5	1.25	10.0
$\frac{1}{4}h$	$h/8$	4.0	15.0	255	6.67	0.39	17.0
$\frac{1}{5}h$	$h/10$	5.0	24.0	624	4.17	0.16	26.0
$\frac{1}{8}h$	$h/16$	8.0	63.0	4095	1.59	0.024	65.0
$\frac{1}{10}h$	$h/20$	10.0	99.0	9999	1.01	0.01	101

\*  $R_o = w_o$  and we assume typical values of  $u = 10^{-4} \frac{\text{cm}}{\text{sec}}$ ,  $\frac{V}{\text{cm}} = 10^2 \text{ V/cm}$ , (so that  $\mu E = 1$ ) and the ratio  $\frac{w_o}{w} = 10^{-2}$ .

throughput at unimpaired resolution suggests, however, that it may be fruitful to move in the opposite direction.

The rectified central velocity increases as  $h^4$ , as seen from equation (15b). It is our aim to choose  $h$  so as to make the rectified velocity  $R_o$  comparable to the currently used vertical velocity in the endless belt (about 4 mm/sec.). Using, for instance, an aqueous buffer at the average temperature of 22°C (from which follows  $\alpha$  and  $\eta$ ), we obtain a velocity in this range for an annulus width  $h = 2.5$  mm. (The maximum temperature difference between the center and walls of the annulus will then be 9°C).

Under these conditions we can use a streak of 0.3 h diameter and still keep the streak divergence below 1%. As compared to currently used injector diameters of 0.5 mm, the throughput will be increased by a factor of 25. Admitting a 4% divergence in a 2.5 mm annulus, we could use an injector of 1 mm i.d. and thus raise the throughput by a factor of roughly 50.

We choose in our example the following parameters:  $J = 6.7 \cdot 10^{-2} \text{ A/cm}^2$ ,  $\Sigma = 7.14 \cdot 10^{-4} \text{ mhos/cm}$ ;  $q = J^2/\Sigma = 1.5 \text{ cal/sec.cm}^3$ ;  $g = 980 \text{ cm/sec}^2$ ,  $\alpha = 2.6 \cdot 10^{-4} \text{ gm/cm}^3/\text{°C}$ ;  $k = 1.32 \cdot 10^{-3} + 3 \cdot 10^{-3} T \text{ °C cal/cm.sec.}$ ;

$$h = 0.25 \text{ cm}; \eta = 9.5 \cdot 10^{-3} \text{ poise.}$$

The value of  $w_o^*$  follows from equation (13):

$$w_o^* = \frac{g \alpha q h^4}{320 \eta k} = 0.38 \text{ cm/sec.}$$

This value is close to the central flow velocity used in a 1.5 mm annulus. With a 2.5 mm annulus a much weaker magnetic field will suffice to obtain the same flow velocity because of the proportionality of  $w^*$  to  $h^4$  at constant magnetic field. Admitting a 5% divergence in a 2.5 mm annulus, we could use an injector of 1 mm i.d. and thus raise the throughput by a factor of roughly 50.

It goes without saying that rectification of the velocity profiles also provides a great increase in resolving power for analytical work. For instance, with an injector of 0.15 mm i.d. in the above example of a 2.5 mm annulus, the predicted streak divergence would be below 0.01%.

#### Applicability of Rectification to the Endless Belt and Fluid Curtain Electrophoresis

We must note that the above possibility of rectifying the horizontal and vertical velocity profiles for simultaneous multiple streak collimation presupposes the capability of generating a lateral laminar flow in addition to the vertical curtain flow. This capability does not exist in the "free flow" apparatus (1) because the sides of the fluid curtain are sealed off by membranes. This enclosure is necessary in order to maintain the vertical flow in the fluid curtain by a pressure gradient. In the "endless fluid belt" system,

on the other hand, the electromagnetic force propelling the fluid is not derived from a gradient field. The sides of the fluid belt are not sealed off by membranes and a horizontal laminar flow can be easily maintained.

The rectification by thermal convection of the velocity profile in the descending path of the endless fluid belt will tend to be canceled by the superposition of thermal convection upon the upward laminar flow in the ascending leg of the annulus. Thus, parabolic divergence of the streak will persist essentially unimpeded after an even number of half-turns of the injected sample. In principle, one could counteract the streak broadening by imposing a corrective modification of the velocity profile in a terminal descending path after an odd number of half-turns. But this would be difficult and less effective than the following simpler approach. One could use only the first descending streak and make up for the loss of the time and path length of the subsequent possible turns by increasing the height of the annulus. Despite a superficial resemblance, this system would differ radically from the "free flow" fluid curtain apparatus by the absence of the lateral membranes and the consequent capability of maintaining a horizontal buffer flow in the separation chamber.

## SUMMARY

Thermal convection and electro-osmotic streaming have been combatted as major obstacles to resolution in continuous-flow electrophoresis. The desire to suppress these effects leads to instrumental design which is not favorable to large preparative throughput as well as to achievement of high resolving power because of streak divergence. Until now it has been possible to minimize streak divergence in continuous-flow deviation electrophoresis for only one electrophoretic component of a mixture by matching the wall zeta potential to the electrophoretic mobility of the singled-out component. It is shown here how a simultaneous collimation of streaks of all components of an electrophoretically heterogeneous mixture can be obtained by superposition of laminar flow, electro-osmotic streaming and thermal convection upon electrophoresis in the separation chamber. An increase in throughput of an order of magnitude can be achieved without a loss in resolution, and at low throughputs in analytical work, an increase in resolution of two orders of magnitude is possible.

## ACKNOWLEDGEMENT

We are indebted to Professor F. Busse of the UCLA Institute of Geophysics for his critical comments and for his simplified derivation of thermal convection velocity distribution with which we replaced ours in this paper.

## REFERENCES

- (1) K. Hannig, H. Wirth, B.H. Meyer and K. Zeiller: Free Flow Electrophoresis I, *Hoppe Seylers Z. f. Physiol. Chem.* 356, 1209-1223, 1975.
- (2) A. Kolin: Endless Belt Continuous-Flow Deviation Electrophoresis in *Electrokinetic Separation Methods*, P. G. Righetti, C. J. van Oss, J. W. Vanderhoff, Eds. (Elsevier-North Holland Medical Press, 1979). (In Press)
- (3) A. Kolin: Cell Separation by Endless Fluid Belt Electrophoresis in *Methods of Cell Separation*, vol. II. N. Catsimpoolas Ed. Plenum Publ. Co., New York, 1979. (In Press)
- (4) A. Kolin: Preparative Electrophoresis in Liquid Columns Stabilized by Electromagnetic Rotation, I, II. *J. of Chromatography* 26, 164-193, 1967.
- (5) M. Smoluchowski: In Handbuch der Elektrizitat und Magnetismus, Vol. 2, L. Graetz, Ed., p. 366 (Barth, Leipzig), 1921.
- (6) A. Kolin: Continuous Electrophoretic Fractionation Stabilized by Electromagnetic Rotation. *Proc. Nat. Ac. Sc.* 46, 509-523, 1960.
- (7) A. Strickler and T. Sacks: Focusing in Continuous-Flow Electrophoresis Systems by Electrical Control of Effective Cell Wall Zeta Potentials in Isoelectric Focusing and Isotachophoresis, N. Catsimpoolas, Ed.,
- (8) A. Kolin: Kinematic Stabilization of Continuous-Flow Electrophoresis Against Thermal Convection. *Proc. Nat. Ac. Sc.* 51, 1110-1117, 1964.
- (9) B. L. Ellerbroek and A. Kolin: Thermal Convection in a Uniformly Heated Fluid between Vertical Parallel Plates. Submitted for Publication 1978.

## TABLE OF SYMBOLS

Symbol	Definition	Units
$z$	distance from midplane between the plates	cm
$\rho$	density of fluid	g/cm <sup>3</sup>
$k$	thermal conductivity	cal/sec/cm/°C
$\sigma$	specific heat	cal/g/°C

$q$	power generation per unit volume	$\text{cal/sec/cm}^3$
$t$	time	$\text{sec.}$
$T$	temperature	$^{\circ}\text{C}$
$T_0$	Temperature at $z = 0$	$^{\circ}\text{C}$
$g$	gravitational field intensity	$\text{cm/sec.}^2$
$p$	pressure	$\text{dynes/cm}^2$
$\eta$	viscosity	poise
$U$	vertical curtain velocity	$\text{cm/sec.}$
$v$	horizontal velocity of fluid	$\text{cm/sec.}$
$\alpha$	temperature coefficient of density	$(\text{gm/cm}^3)^{(\text{ }^{\circ}\text{C})^{-1}}$
$v_o$	central maximum vertical velocity	$\text{cm/sec.}$
$v_h$	central maximum horizontal velocity	$\text{cm/sec.}$
$h$	distance between the vertical plates	$\text{cm.}$
$W$	Electro-osmotic mobility = Electro-osmotic velocity at the wall in a unit electric field	$\frac{\text{cm}}{\text{sec.}}/\frac{\text{V}}{\text{cm}}$
$\mu$	electrophoretic mobility	$\frac{\text{cm}}{\text{sec.}}/\frac{\text{V}}{\text{cm}}$
$E$	electric field intensity	$\text{V/cm}$
$\Sigma$	electrical conductivity of the buffer	$\text{mhos/cm}$

### KEY WORDS

Electrophoresis; Endless belt electrophoresis; Deviation electrophoresis; Free-flow electrophoresis; Streak collimation; Electrophoretic resolving power; Electrophoretic throughput; Thermal convection; Electro-osmosis.